Gamma ray point source search by GRAPES-3 experiment

A.Oshima[*], **S.R.Dugad**[*], **T.Fujii**[†], **U.D.Goswami**[*], **S.K.Gupta**[*], **Y.Hayashi**[†], **N.Ito**[†],
P.Jagadeesan[*], **A.Jain**[*], **S.Karthikeyan**[*], **S.Kawakami**[†], **H.Kojima**[‡], **T.Matsuyama**[†],
M.Minamino[†], **H.Miyauchi**[†], **P.K.Mohanty**[*], **S.D.Morris**[*], **P.K.Nayak**[*], **T.Nonaka**[†],
S.Ogio[†], **T.Okuda**[†], **B.S.Rao**[*], **K.C.Ravindran**[*], **M.Sasano**[†], **K.Sivaprasad**[†],
H.Tanaka[†], **S.C.Tonwar**[*], **E.Usui**[†], **Y.Yamashita**[†]

[*]*Tata Institute of Fundamental Research*
[†]*Osaka City University, Japan*
[‡]*Aichi Institute of Technology*

Abstract. **The GRAPES-3 experiment at Ooty in India, is an air shower array of about 300 plastic scintillator detectors, and a large area (560 m^2) tracking muon detector with 1 GeV energy threshold. The detectors are deployed on a hexagonal pattern with inter-detector distance of 8m. A good angular resolution is required for the search of gamma-ray point sources which is also one of the main objectives of the GRAPES-3 experiment. An angular resolution of the array is $\leq 1°$ above a primary energy 20 TeV. The large area tracking muon detector is used to measure the muon component of each detected showers. The huge number of EAS due to charged primary cosmic rays is the main background for the gamma ray point sources search. Since the EAS induced by cosmic rays contain larger number muons due to their hadronic interactions, we may distinguish primary gamma-ray induced events from the hadron induced showers, by using the information from the muon detectors. A gamma-ray signal from the direction of the CRAB nebula has been obtained from the GRAPES-3 array which will be presented and discussed.**

Keywords: **cosmic ray,gamma ray, Crab Nebula**

I. INTRODUCTION

The discovery of the pulsars in the 1960s further added to the interest in particle acceleration processes associated with supernovae, since the pulsars themselves were shown to be capable of directly accelerating particles to TeV energies and beyond. Among the many known pulsars and the associated supernova remnants, the CRAB pulsar and its associated nebula have been among the most-studied astronomical objects at all wavelengh in the electromagnetic spectrum.
Successful models for the production of γ-rays up to GeV energies, invoke the acceleration of the charged particles in the pulsar wind by the shock front to relativistic energies, and the production of the γ-rays occurs through the synchrotron and curvature radiation processes. The γ-ray energy spectrum of the CRAB nebula has been measured up to TeV energies by the pioneering observations of the Whipple group [**?**]. Detailed studies on the energy spectrum in the TeV energy region by the recent high resolution imaging Ĉerenkov telescopes such as MAGIC, HESS and VERITAS etc., have enabled highly successful modeling of the acceleration and γ-ray generation processes occurring in the CRAB nebula. These models visualize the production of the γ-rays, through inverse Compton scattering of the synchrotron photons by the synchrotron-emitting highly relativistic electrons in the shock region. A fit to the TeV spectrum requires the acceleration of particles up to energies $\sim 10^{15}$ eV.

It is expected that a significant part of the energy loss from the pulsar would be in the form of the hadronic component of the pulsar wind. The γ-rays produced through the decay of neutral pions ($\pi^°$) via hadronic interactions, would have significantly different energy spectrum than the photons produced by the inverse Compton scattering from the electrons. Since the lifetime of TeV electrons in the nebular magnetic field decreases very rapidly with increasing energy, a steepening of the energy spectrum is expected in the 10-100 TeV region. On the other hand, the spectrum of the γ-rays produced via $\pi^°$ decays may extend the energy spectrum beyond 10 TeV, without much change in the slope. Therefore, there is considerable interest, in exploring the shape of the energy spectrum in the 10-100 TeV region, in order to determine the relative contributions of these two competing processes for the production of the γ-rays in the CRAB nebula.
We present here, the results from a 5-year study of the showers arriving from the direction of the CRAB nebula, using the muon-poor criterion for their selection as γ-ray candidate events.

II. GRAPES-3 EXPERIMENT

The experimental system of the GRAPES-3 (**G**amma **R**ay **A**stronomy at **P**eV **E**nergy**S** Phase-**3**) experiment consists of a densely packed array of scintillator detectors and a large area tracking muon detector. The EAS array consists of 257 plastic scintillator detectors shown in Fig. 1, each of 1 m^2 in area. These detectors are deployed with an inter-detector separation of only 8 m. The array is being operated at Ooty in south India (11.4°N, 76.7°E, 2200 m altitude).

In order to achieve the lowest possible energy threshold, a simple 3-line coincidence of detectors has been used to generate the Level-0 trigger, which acts as the fast GATE and START for the analog to digital and time to digital converters (ADCs and TDCs), respectively. As expected, this trigger selects a large number of very small and local showers and also larger showers whose cores land very far from the physical area of the array. Therefore, it is also required that at least 10 out of the inner 127 detectors should have triggered their discriminators within 1 μs of the Level-0 trigger. This Level-1 trigger with an observed EAS rate of 13 Hz is used to record the charge (ADC) and the arrival time (TDC) of the pulses from each detector [4]. The pulse charge is later converted into the equivalent number of minimum-ionizing particles (MIPS) using the most probable charge for a single MIP measured using the trigger from a small area (20×20 cm^2) scintillation counter telescope.

The 560 m^2 GRAPES-3 muon detector [9] consists of 4 super-modules in Fig. 2 , each in turn having 4 modules. Each module with a sensitive area of 35 m^2 consists of a total of 232 proportional counters (PRCs) arranged in 4 layers, with alternate layers placed in orthogonal directions. Two successive layers of PRCs are separated by 15 cm thick concrete. The energy threshold of 1 GeV for vertical muons, has been achieved by placing a total of 15 layers of concrete blocks (total absorber thickness $\sim$550 g.cm^{-2}) above the Layer-1. The concrete blocks have been arranged in the shape of an inverted pyramid to provide adequate shielding up to a zenith angle of $45°$.

One of the most critical parameter in the search for point sources of cosmic γ-rays, using a particle detector array is good angular resolution. This requires an accurate determination of the relative arrival time of the shower front at various detectors. The high density of the detectors in GRAPES-3 enabled an angular resolution of $0.7°$ to be obtained at energies as low as 30 TeV. Angular resolution of the GRAPES-3 was estimated by 2-D Gaussian fit to the Moon shadow data.

III. DATA AND ANALYSIS

A total of 1.9×10^9 showers have been collected over a total live time of 11.9×10^7 s, spread over a 5-year period, from 2000 to 2004. For each EAS, the core location, the shower age 's' representing the steepness of the Nishimura-Kamata-Greisen (NKG) lateral distribution function and the shower size N_e have been determined using the observed particle densities, following the minimization procedure discussed in detail by Tanaka et al [6]. Also, for each shower, the zenith (θ) and the azimuth (ϕ) angles have been calculated using the time information from the TDCs, also following the minimization procedure described by Tanaka et al [6]. It is very difficult to observe the tiny flux of γ-rays from various interesting astrophysical sources in the sea of nuclear cosmic rays whose direction has been randomized
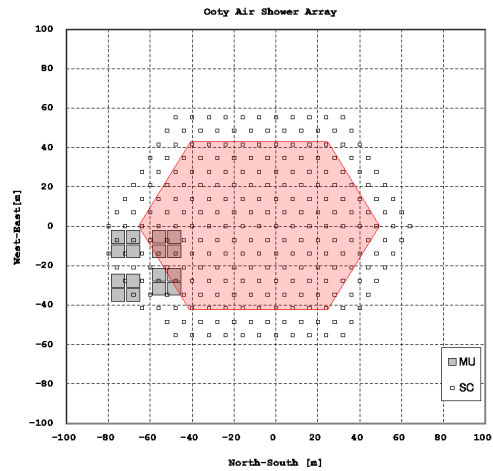

Fig. 1.   The GRAPES-3 experimental system with 257 scintillator detectors and 16 muon detector modules
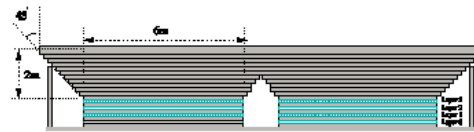

Fig. 2.   A muon station has four muon detector modules each consisting of 232 proportional counters. There are four muon stations inside the air shower array (Fig. 1).
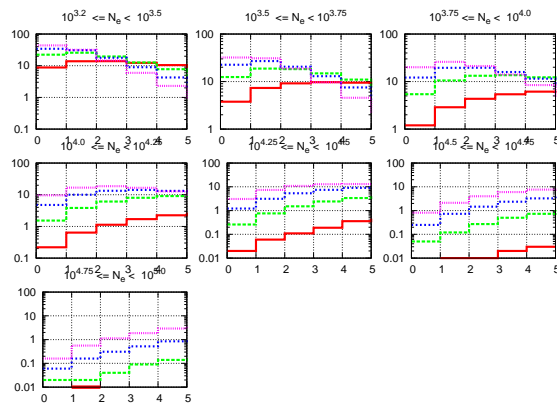

Fig. 3.   Distribution of the number of muons accompanying the observed air shower for each shower size range.

by the interstellar magnetic field. At higher energies, where observations have to be necessarily made with particle detector arrays at high altitudes, the muon content of showers offers itself as a possible parameter to discriminate against showers initiated by nuclear cosmic rays. Fig. 3 shows the GRAPES-3 observations on the muon content of showers.

Fig. 4 shows the distribution of the number of showers in various annular regions centered on the direction of the Crab nebula for the complete data set of nearly 5 years, for $N^e \geq 10^{4.0}$ which satisfied the 'zero-muon' and 'muon-poor' criteria. It is interesting to note a small
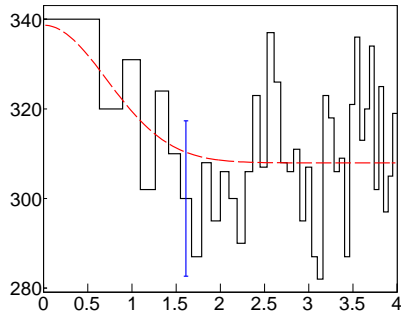
Fig. 4. Distribution of the number of showers in various annular regions centered on the direction of the Crab nebula for a sub-set of the complete set of showers , which satisfy the 'zero-muon' and 'muon-poor' criteria.

excess (2.1σ) flux from within 2° of the Crab nebula from a Gaussian fit to the data plotted in Fig. 4.

It is evident that the statistical significance of the excess from the direction of the Crab nebula for the 'zero-muon' and 'muon-poor' showers is not large and not beyond the possibility of being a statistical fluctuation. However, it is still of considerable interest to compare the observed flux with other observations at TeV-PeV energies, specially in view of the fact that the present results possibly represent the first positive detection of the gamma ray flux from the Crab nebula using the 'zero-muon' and 'muon-poor' criteria with one of the largest muon detectors used for this purpose. It may be noted here that the background flux, required for estimating the excess from the direction of the Crab nebula is rather well-determined and agrees well among the three observation regions.

In general, the integrated intensity of gamma rays from an astronomical object can be expressed as follows:

$$I = \int_{E_t}^{E_c} \frac{dN}{dE} dE \qquad (1)$$

where E_t is the effective threshold energy for detection of gamma rays with the GRAPES-3 array and E_c is the assumed cut-off energy for the energy spectrum. E_c is being taken to be 10^{14} eV here. The differential intensity can be assumed to be given by the relation:

$$\frac{dN}{dE} dE = I_0 \left(\frac{E}{E_0} \right)^{-\alpha} \qquad (2)$$

where α is the power-law exponent for the spectrum in the 10-100 TeV energy range and I_0 is the differential intensity at a value E_0 for the γ-ray energy. Combining the above two equations, the integrated intensity I is obtained as follows,

$$I = \int_{E_1}^{E_2} I_0 \left(\frac{E}{E_0} \right)^{-\alpha} dE \qquad (3)$$

$$= \frac{I_0 E_0}{-\alpha + 1} \left[\left(\frac{E_c}{E_0} \right)^{-\alpha} - \left(\frac{E_1}{E_0} \right)^{-\alpha} \right] \qquad (4)$$
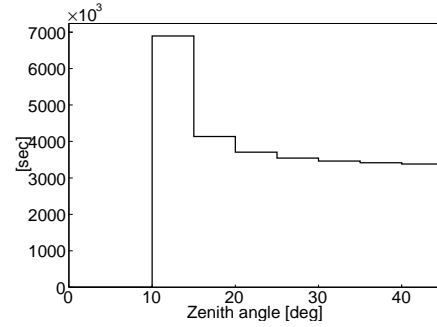

Fig. 5. Exposure time for the Crab nebula as a function of the zenith angle in 5° intervals.

The observed flux from the Crab nebula, integrated over the time interval, between times t1 and t2, may be written as,

$$I = \int_{E_t}^{E_c} \int_{t_1}^{t_2} \frac{dN}{dE} A_{eff}(E, \theta(t)) dt dE \qquad (5)$$

where A_{eff}(E,θ(t)) is the effective area of the shower array for the γ-ray energy E and θ(t) is the zenith angle of the Crab Nebula at time t.

Fig. 5 shows the variation of the exposure time for the Crab nebula with the zenith angle θ(t) in 5° intervals. we have converted the shower size N_e into the energy of the primary protons, using the CORSIKA Monte Carlo simulation program, version 6.500 in Fig. 6 [8]
Using the values of the exposure times for various zenith angles shown in Fig. 5 and converting the observed shower size to primary energy of gamma rays using the energy-size relation shown in Fig. 6, the integral flux values have been determined for 5 values of the primary energy. For example, the integral flux above an energy threshold of of 9 TeV is found to be (5.08 ± 2.67) $\cdot 10^{-13} cm^{-2} s^{-1}$ and (6.92 ± 2.87) $\cdot 10^{-14} cm^{-2} s^{-1}$ for energy above 30 TeV. These results are plotted in Fig. 7 for obtaining the gamma ray energy spectrum for the Crab nebula. The power-law index for the energy spectrum determined from these observations is 1.70±0.06 over the energy range, 9–70 TeV. In the same figure are also shown various other measurements, most of them obtained from observations with imaging atmospheric Cherenkov telescopes, except for the result from Tibet which was also based on observations with particle detector array.
It is interesting to see from Fig. 7 that a single power-law seems to fit all the measurements from ∼500 GeV to energies ∼100 TeV and there is no evidence to suggest any steepening of the spectrum, at least upto energy ∼100 TeV.

IV. DISCUSSION

The results presented in Fig. 7 also show that the measurements right up to energy ∼ 100 TeV remain consistent with the predictions of the 'inverse-Compton
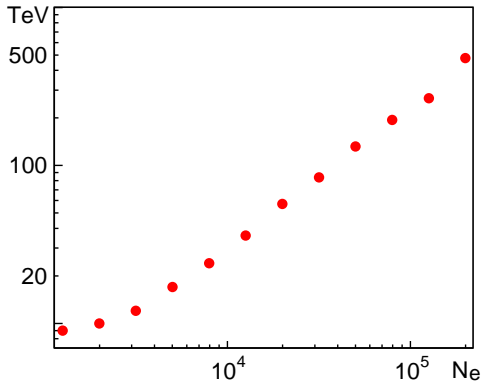
Fig. 6.   The x-axis shows the shower size N_e and corresponding primary proton energy in TeV, is shown on the y-axis.

scattering' model which requires only the acceleration of high energy electrons to PeV energies in the CRAB nebula. There is still no pressing need to invoke the presence of PeV energy hadronic cosmic rays in the CRAB nebula. However, any observation extending the spectrum to energy $\sim$ 1000 TeV without significant steepening is likely to make a strong case for a large contribution of the hadronic cosmic rays to the observed γ-ray flux. In this context, it is relevant to mention here that the GRAPES-3 array is expanded to increase the collection area and the size of the muon detector is also being increased. These additions to the GRAPES-3 system should help in extending the observations on the gamma ray energy spectrum for the CRAB nebula to energies $\sim$ 1000 TeV.

V. SUMMARY

We have analyzed air shower data collected by the GRAPES-3 experiment over a 5-year period from 2000 to 2004. A search for an excess flux due to γ-rays from the CRAB nebula over the complete data set has yielded negative result. However, using the discriminating power of the muon component of air showers to improve the signal to background, we have observed an excess flux in showers selected with 'zero-muon' and 'muon-poor' criteria. These observations yield an integral flux of $(5.08 \pm 2.67) \cdot 10^{-13} cm^{-2} s^{-1}$ above an energy threshold of 9 TeV and $(6.92 \pm 2.87) \cdot 10^{-14} cm^{-2} s^{-1}$ for energy above 30 TeV. The observed flux is in good agreement with the large-angle observations by the CANGAROO collaboration with atmospheric Ĉerenkov telescope and also with the results reported by the Tibet AS/γ collaboration. The energy spectrum shows a single power-law fit over the broad energy range, 500 GeV to 100 TeV, consistent with the expectations from the 'Inverse-Compton scattering' model for the acceleration of electrons and production of γ-rays in the CRAB nebula. An on-going expansion of the GRAPES-3 particle array as well as the enlargement of the muon detector is expected to help in the extension of observations on the energy spectrum to energies $\sim$ 1000 TeV which would permit a distinction
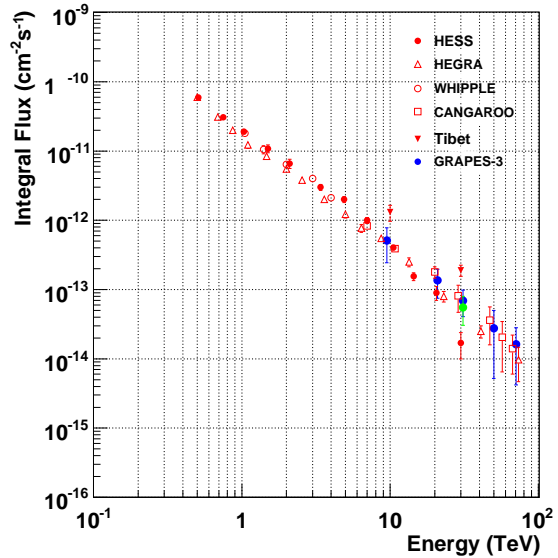

Fig. 7.   Integral energy spectrum of gamma rays from the Crab nebula. The flux values obtained from the present experiment are in good agreement with the results given by the CANGAROO and Tibet AS/γ collaborations. However, the flux observed by the HESS collaboration is almost 50% larger than the values obtained from the GRAPES-3 experiment.

between electron and hadronic processes for the γ-ray production in the CRAB nebula.

REFERENCES

[1] S.K. Gupta et al., Astrophys. Space Sci. 115 (1985) 163.
[2] S.K. Gupta, et al., J. Phys. G: Nucl. Part. Phys. 17 (1991) 1271.
[3] D.E. Alexandreas et al., Phys. Rev. D 43 (1991) 1735.
[4] S.K. Gupta et al., Nucl. Instr. Methods A 540 (2005) 311.
[5] K. Greisen, Ann. Rev. Nuc. Sci. 10 (1960) 63.
[6] H. Tanaka et al., GRAPES-3 Preprint (2006).
[7] S.C. Tonwar, Workshop on Techniques in UHE γ-ray Astronomy, La Jolla, Eds: R.J. Protheroe & S.A. Stephens, Univ. of Adelaide (1985) 40.
[8] http://www-ik.fzk.de/corsika
[9] Y. Hayashi et al., Nucl. Instr. Methods A 545 (2005) 643.